Observation of Interaction between Fast Ions and Turbulence in Large Helical Device*)

Hikona SAKAI[1)], Kenji TANAKA[1,2)], Toshiki KINOSHITA[1)] and Kunihiro OGAWA[2,3)]

[1)]*Interdisciplinary Graduate School of Engineering Sciences, Kyushu University, Kasuga, Fukuoka 816-8580, Japan*
[2)]*National Institute for Fusion Science, Toki, Gifu 509-5292, Japan*
[3)]*The Graduate University for Advanced Studies, SOKENDAI, Toki, Gifu 509-5292, Japan*

(Received 9 January 2023 / Accepted 11 June 2023)

Systematic experiments were carried out in the 23rd Large Helical Device experiment campaign to explore the interaction between fast ions and ion-scale turbulence focusing on the impact of varying the power of the neutral beam (NB) injection. During the NB heating, two distinct phases of turbulence reduction were observed. The first phase was a transient reduction of about 10 msec immediately following the initiation of the NB injection. This reduction in turbulence was noticeable even while the electron density and temperature profiles remained nearly unchanged. The second phase involved a continuous reduction that maintained a lower turbulence level throughout the duration of the NB injection. The physics mechanisms underlying these phenomena are not fully understood yet. However, it is likely that two distinct processes of turbulence stabilization, each corresponding to the transient and continuous reduction phases, are at work due to the influence of the fast ions.

Keywords: plasma, turbulence, fast ions, interaction

DOI: 10.1585/pfr.18.2402069

1. Introduction

Comprehending the interaction between fast ions and turbulence is crucial for predicting future fusion reactor operations. Fast ions generate macroscopic magnetohydrodynamics (MHD) instabilities such as the toroidal Alfvén eigenmodes (TAE), but their interaction with microscopic turbulence is not well understood. Recent findings from the Joint European Torus (JET) suggest that fast ions stabilize ion temperature gradient (ITG) turbulence and relax the stiffness of the ion temperature profile due to the fast ion pressure [1,2]. Moreover, JET findings also indicated that the fast ion-driven TAE mode acted as a zonal flow suppressing the ITG turbulence [3, 4]. However, evidence directly supporting turbulence reduction has been scarce and was only reported in [4].

This paper presents the results from a systematic study of the interaction between fast ions and micro-turbulence. The experiments were conducted on the Large Helical Device (LHD) at the National Institute for Fusion Science. In order to analyze the effects of fast ions on turbulence, it was vital to distinguish between the direct effects of the fast ions and the effects of changes in density and temperature profiles due to heating. To ensure this, short pulses (~80 msec) of neutral beams (NBs) were injected to prevent altering the plasma profile. As a result, two distinct phases of turbulence reduction were identified: an initial, strong transient reduction following the NB injections, and a second, modest and continuous reduction maintained throughout the NB injections.

2. Experimental Results

The LHD is a heliotron-type device [5]. It contains a set of two superconducting helical winding coils and three pairs of superconducting vertical coils, which generate a helically shaped magnetic flux surface [5]. For NB heating, three parallel-injected negative ion-based NBs (NNBs; NB#1, 2, 3) and two perpendicularly injected positive ion-based NBs (PNBs; NB#4, 5) are used. The NNBs predominantly heat electrons, while the PNBs predominantly heat ions. The two PNBs (NB#4, 5) were utilized for this experiment, with each possessing slightly different injection power and energy. NB#4 and NB#5 had injection powers of 8 MW and 7 MW, respectively, and injection energies of 55 keV and 62 keV, respectively. Each PNB comprises four ion sources, and the power can be adjusted by operating two or four ion sources. Additionally, there are five gyrotrons (three at 77 GHz and two at 154 GHz) for electron cyclotron resonance heating (ECRH). The magnetic configuration employed in these experiments was the inward-shifted configuration, with a magnetic axis position at 3.6 m and a toroidal magnetic field of 2.75 T. This configuration is most frequently used due to its efficient performance [6].

In this study, we injected short pulses (80 msec wide) of deuterium PNBs into a deuterium plasma sustained by 2 MW 154 GHz second harmonic ECRH. The short pulse (~80 msec) injection was chosen to maintain stable density

author's e-mail: h.sakai@triam.kyushu-u.ac.jp
*) This article is based on the presentation at the 31st International Toki Conference on Plasma and Fusion Research (ITC31).

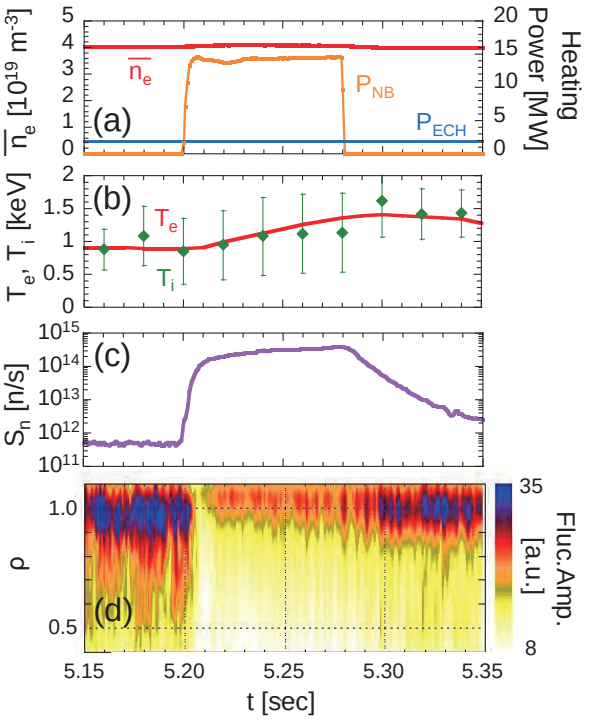

Fig. 1 Time evolutions of (a) line-averaged electron density and heating power, (b) electron temperature and ion temperature, (c) total neutron emission rate, and (d) spatial structure of turbulence amplitude (shot 173726).

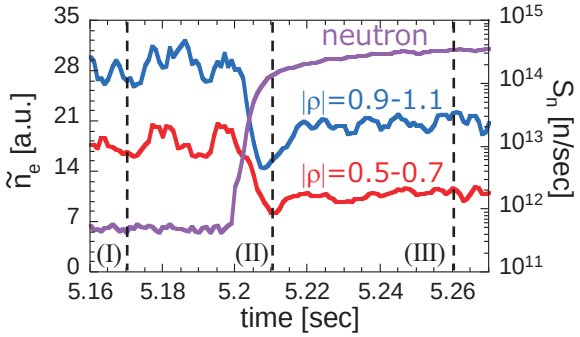

Fig. 2 Expanded view of turbulence amplitude in the core (ρ = 0.5 - 0.7) and edge (ρ = 0.9 - 1.1) regions and total neutron emission rate.

and temperature profiles. Ion-scale turbulence was measured using two-dimensional phase contrast imaging (2D-PCI) [7]. The 2D-PCI measures turbulence with a spatial resolution of approximately 10 - 30% of the minor radius and turbulence values of k = 0.1 - 1 mm^{-1}, f = 20 - 500 kHz. The injection power of the PNBs was varied by using a combination of the two PNBs.

Figure 1 illustrates the time progression with two PNB injections. Figure 1 (a) plots the line-averaged electron density ($\overline{n_e}$), the total heating power of a NB (P_{NB}) and ECH (P_{ECH}). Figure 1 (b) shows the electron temperature (T_e), measured by electron cyclotron emission (ECE), and ion temperature (T_i) ascertained through Doppler broadening using the Argon resonance line at 0.3949 nm of Ar^{16+}, i.e., Ar XVII 1 s^2 ^{1}S$_0$-1s2p ^{1}P$_1$ [8,9]. The electron temperature data gathered at ρ = 0.6 was chosen for comparison with the turbulence data gathered by 2D-PCI. Even though the ion temperature determined through Argon Doppler broadening was an integrated measurement, the radiation intensity was primarily centered on the plasma center, where the radiation intensity is strongest. These measurements allowed us to capture the rapid changes following PNB injections. In Fig. 1 (c), we estimated the total neutron emission rate using a ^{235}U fission chamber (FC) [10]. These neutrons were produced by the fusion reaction between the beam deuterium and bulk deuterium, thus their total emission rate represents the generation of fast ions from the deuterium beams. As depicted in Fig. 1 (c), the total neutron emission rate spiked after the PNB injections, remaining steady throughout the PNB pulses before decreasing gradually post-injection due to the slowing down process of the beam fast ions. Figure 1 (d) represents the time evolution of ion-scale turbulence as measured by 2D-PCI. The turbulence signal was captured at 1 μsec sampling, and spatial profiles were computed every 1 msec using the magnetic shear technique and the maximum entropy method (MEM) [7, 11].

As evident in Fig. 1 (d), turbulence decreased immediately after PNB injections at 5.2 sec, and lower turbulence amplitude persisted until the PNBs were turned off at 5.28 sec. Turbulence then increased during the slowing down phase, returning to levels pre-PNB injections. The recovery timeframe was consistent with the decay time of the total neutron emission rate. It should be emphasized that we observed two phases of turbulence reduction. The first, a significant reduction immediately post-PNB injections, is termed "the first transient reduction" in this paper. The second, a modest reduction sustained during the PNB injections, is termed "the second continuous reduction" in this paper. Figure 2 provides a more detailed view of these two phases.

Figure 2 compares the temporal evolution of turbulence amplitude in the core (ρ = 0.5 - 0.7) and edge (ρ = 0.9 - 1.1) regions with the variation in the total neutron emission rate. As shown in Fig. 2, turbulence amplitude began to decrease immediately after the PNB injections at t = 5.2 sec, while neutron emission rates began to increase. The turbulence amplitude reached a minimum at t = 5.21 sec, when the increase in neutron emission rates had saturated. This marked the first, strong reduction. Turbulence did increase post this point but never returned to its pre-PNB injection value, maintaining a lower level after t = 5.22 sec for the duration of the PNB injections. This period represents the second, continuous reduction phase. This response was observed in both core (ρ = 0.5 - 0.7) and edge (ρ = 0.9 - 1.1) regions.

Figure 3 shows the n_e, T_e, and electron pressure (P_e) profiles at three specific points in time:

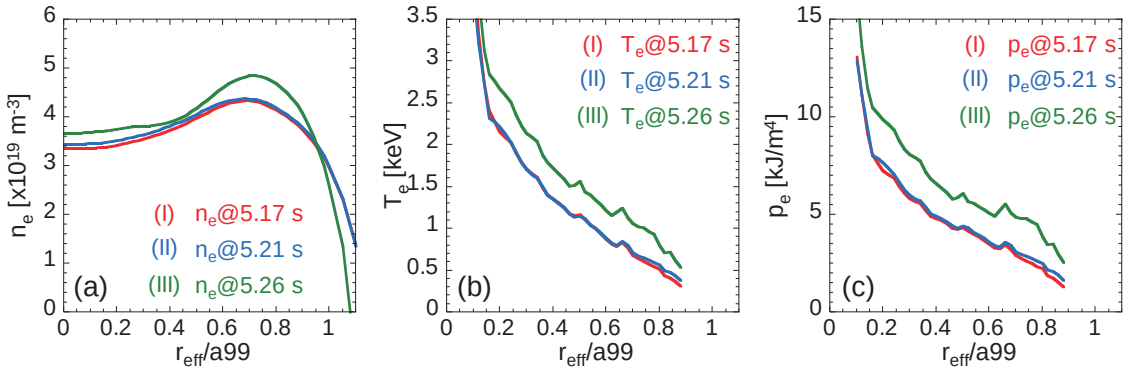

Fig. 3 Profiles of (a) electron density, (b) electron temperature, and (c) electron pressure. The red, blue, and green lines represent specific points in time: just before NB injection (I, 5.17 s), the moment of minimum amplitude (II, 5.21 s), and the point when turbulence amplitude increases but is lower before NB injection (III, 5.26 s). The density profiles were evaluated by the Abel inversion of a FIR interferometer [12, 13], while the temperature profiles were derived from ECE.

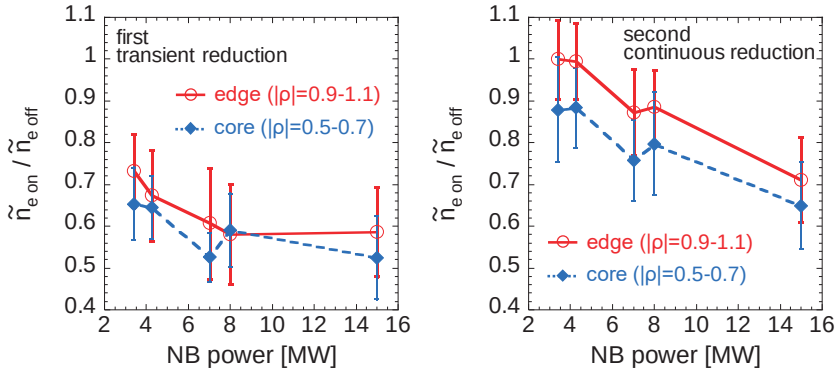

Fig. 4 NB heating power dependence of turbulence suppression ratio. The first transient reduction represents the ratio of turbulence amplitudes at timing II to timing I, whereas the second mode reduction indicates the ratio of turbulence amplitudes at timing III to timing I. NB power of 4.3 and 8.0 MW were produced by NB#4, NB power of 3.4 and 7.0 MW were generated by NB#5, and a NB power of 15 MW was produced by both NB#4 and NB#5.

I. Before the NB injection at t = 5.17 sec
II. After the NB injection and when the turbulence amplitude is at its minimum at t = 5.21 sec
III. After the NB injection and after the turbulence amplitude increases and maintains a modest reduction of turbulence at t = 5.26 sec.

As illustrated in Fig. 3, all profiles remained unchanged between timings I and II, indicating that the first transient reduction was not due to differences in profiles. Therefore, this reduction was due to the fast ions produced by the PNB injections. Furthermore, the timescale of turbulence reduction (t = 5.20 - 5.21 sec) aligns with the increase in total neutron emission rate as depicted in Fig. 2. This strongly suggests that the first transient reduction was caused by the fast ions produced by PNB injections.

During the later phase from timing II to III, the n_e, T_e and P_e increased slightly at $\rho < 0.9$. The changes in T_e and P_e were particularly significant. Consequently, we cannot completely disregard the effect of profile variation. However, as depicted in Fig. 1 (b), the T_e gradually increased during the PNB injections, while the turbulence amplitude remained virtually unchanged between timings II and III, as shown in Fig. 2. Thus, there is still a possibility that fast ions contributed to the second continuous reduction.

Finally, we investigated the PNB power dependence of turbulence reductions. Here, we define the turbulence reduction ratio as $\tilde{n}_{e\ ON}/\tilde{n}_{e\ OFF}$, where $\tilde{n}_{e\ ON}$ is turbulence amplitude with PNB injections and $\tilde{n}_{e\ OFF}$ is that before starting PNB injection. We define the first transient reduction ratio as the amplitude ratio at timings II to I, and the second continuous reduction ratio as the turbulence amplitude at timings III to I.

We estimated the ratios for both the core (ρ = 0.5 - 0.7) and edge (ρ = 0.9 - 1.1) regions over a 10 msec time window at each timing. We derived the error bars from the statistical distribution of amplitude for each analysis time window. As the 2D-PCI measures both the upper and lower sides of the equatorial plane [7], we performed evaluations on both sides.

In this study, we scanned PNB power in five different cases: 3.4, 4.3, 7.0, 8.0, and 15 MW. The result is depicted in Fig. 4. We found differences in power dependence of re-

duction ratios between the first transient reduction and the second continuous reduction. The first transient reduction was clearly enhanced from 3.4 to 8.0 MW. However, the reduction did not change significantly from 8.0 to 15 MW. Also, the difference in turbulence reduction between the core and edge regions was not evident. On the other hand, the second continuous reduction was enhanced with the increase in NB power. The reduction in the core region was higher than that in the edge region. The differing power dependencies in the first transient and second continuous reductions also suggested that different physical mechanisms were at play in the two reduction phases.

3. Discussion and Summary

We experimentally investigated the interaction between fast ions and ion-scale turbulence in LHD. We found two distinct reduction phases during the injection of the PNBs. The first transient reduction occurred just after the PNB injection began and lasted for 10 msec, with constant n_e and T_e profiles. The global energy confinement time is about 100 msec, which is significantly longer than the first transient reduction. This finding supports the idea that the first transient reduction is not due to changes in confinement, but due to the injection of fast ions. The transient reduction of turbulence was also observed due to the loss of fast ions, which triggered energetic particle-driven interchange (EIC) mode [14–16]. In EIC mode, the transient reduction of turbulence lasted 1 msec, which was much shorter than our results. Additionally, the reduction was caused by the strong E_r and/or shear formation [15, 16]. In contrast, during these experiments, the transient reduction of turbulence was caused by the injection of fast ions rather than their loss. The underlying physical mechanisms might differ. However, it is possible that strong E_r and/or E_r shear was transiently formed just after the PNB injection. Further measurements of E_r are needed to confirm this hypothesis.

The first transient reduction does not significantly impact total transport due to its inability to maintain reduced turbulence. The second continuous reduction, which sustains suppressed turbulence during the gradual increase of ion and electron temperatures is more consequential for transport. The difference in the timescales of turbulence and temperature changes substantiates the idea that the second continuous reduction is attributable to the impact of fast ions.

In accordance with tokamak theory, ITG stabilization can be attributed either to the electromagnetic effects of fast ion pressure [1, 2], or the role of the TAE mode as a zonal flow [3, 4]. In these experiments, the TAE mode was not observed in the magnetic probe signal, which points to the electromagnetic effects of fast ion pressure as a possible explanation. First principle theoretical gyrokinetic studies have reported that the ratio of fast ion density and temperature gradient determines stabilization. Specifically, the ITG is stabilized for $L_{nF}/L_{TF} < 1$ and destabilized for $L_{nF}/L_{TF} > 1$, where the L_{nF} and L_{TF} are the density and temperature scale length of fast ions, respectively [17]. Therefore, future investigations should include a gyrokinetic study that takes into account the fast ion pressure profile, along with further experimental research.

Acknowledgement

The authors would like to thank the LHD experimental group for excellent operation of LHD. LHD data can be accessed from the LHD data repository at https://www-lhd.nifs.ac.jp/pub/Repository_en.html. This study was supported by the NIFS grant NIFS21ULHH013 and NIFS22ULHH013, JSPS grant 21H04458, the Junichi Miyamoto Hydrogen Research Award, and NIFS Research Fellows program.

[1] J. Citrin *et al.*, Phys. Rev. Lett. **111**, 155001 (2013).
[2] N. Bonanomi *et al.*, Nucl. Fusion **59**, 126025 (2019).
[3] S. Mazzi *et al.*, Nat. Phys. **18**, 776 (2022).
[4] S. Mazzi *et al.*, Plasma Phys. Control. Fusion **64**, 114001 (2022).
[5] M. Osakabe *et al.*, Nucl. Fusion **62**, 042019 (2022).
[6] H. Yamada *et al.*, Nucl. Fusion **45**, 1684 (2005).
[7] K. Tanaka *et al.*, Rev. Sci. Instrum. **79**, 10E702 (2008).
[8] S. Morita *et al.*, Rev. Sci. Instrum. **74**, 2036 (2003).
[9] M. Goto *et al.*, Plasma Fusion Res. **5**, S1040 (2010).
[10] M. Isobe *et al.*, Rev. Sci. Instrum. **85**, 11E114 (2014).
[11] C.A. Michael *et al.*, Rev. Sci. Instrum. **86**, 093503 (2015).
[12] K. Tanaka *et al.*, Plasma Fusion Res. **3**, 050 (2008).
[13] Y. Ohtani *et al.*, Plasma Phys. Control. Fusion **62**, 025029 (2020).
[14] X.D. Du *et al.*, Phys. Rev. Lett. **114**, 155003 (2015).
[15] K. Tanaka *et al.*, Nucl. Fusion **57**, 116005 (2017).
[16] C.A. Michael *et al.*, Nucl. Fusion **58**, 046013 (2018).
[17] G. Wilkie *et al.*, Nucl. Fusion **58**, 082024 (2018).